

# Numerical Simulation of Dissolved Silica in the San Francisco Bay

David H. Peterson, "John F. Festa  
and T. John Conomos"

<sup>a</sup> U.S. Geological Survey, 345 Middlefield Road, Menlo Park, CA 94025 U.S.A.

<sup>b</sup> Atlantic Oceanographic and Meteorological Laboratories, National Oceanographic and Atmospheric Administration, 15 Rickenbacker Causeway, Virginia Key, Miami, FL 33149, U.S.A.

Received 28 March 1977 and in revised form 26 July 1977

**Keywords:** partially mixed estuary; silica; river flow; simulation; numerical model; San Francisco Bay

A two-dimensional (vertical) steady-state numerical model that simulates water circulation and dissolved-silica distributions is applied to northern San Francisco Bay. The model (1) describes the strong influence of river inflow on estuarine circulation and, in turn, on the biologically modulated silica concentration, and (2) shows how rates of silica uptake relate to silica supply and mixing rates in modifying a conservative behavior. Longitudinal silica distributions influenced by biological uptake (assuming both vertically uniform and vertically decreasing uptake situations) show that uptake rates of 1 to 10  $\mu\text{g-at. l}^{-1} \text{ day}^{-1}$  are sufficient to depress silica concentrations at river inflows of 100–400  $\text{m}^3 \text{ s}^{-1}$ , respectively, and that the higher rates appear ineffective at inflows above 400  $\text{m}^3 \text{ s}^{-1}$ . The simulations further indicate that higher silica utilization in the null zone is not essential to depress silica concentrations strongly there. Advective water-replacement times at river inflows of 400, 200 and 100  $\text{m}^3 \text{ s}^{-1}$  are computed to be less than 25, 45 and 75 days, respectively, for a 120-km estuary-river system.

## Introduction

Physical processes control the distributions and behavior of many biologically reactive substances in estuaries. Although there are difficult problems which require increased understanding of the factors controlling currents and salinity distributions (cf. Dyer, 1976), our present knowledge of estuarine dynamics is sufficient for modelling some general features of biologically reactive substances. Seasonal variations in water chemistry and phytoplankton abundance in San Francisco Bay estuary (Peterson *et al.*, 1975a) appear to be closely related to the general water circulation patterns in the estuary. In this paper we contribute some understanding of water-circulation effects on nonconservative (biological and chemical) distributions in partially mixed estuaries. We describe a steady-state numerical model of dissolved silica and apply it to the seasonal silica variations in northern San Francisco Bay, estimating silica-utilization rates which produce nonconservative distributions.

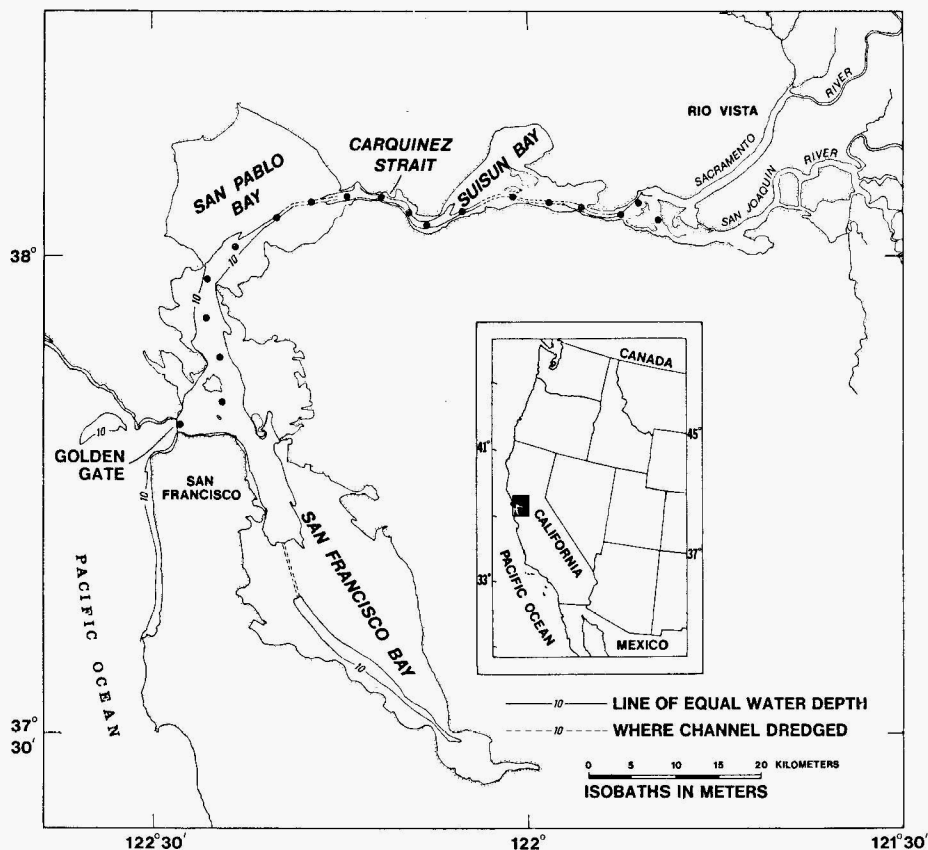


Figure 1. San Francisco Bay system and environs. The study area is between Rio Vista and Golden Gate, the entrance to the ocean. All field data presented herein were collected at mid-channel stations.

Seasonal differences in water circulation in the northern bay (Figure 1) are created primarily by high (winter) and low (summer) river flow. Although average wind speeds are higher in summer than winter (Conomos & Peterson, 1976) the seasonal effect in this portion of the system is probably secondary to that of river inflow. We have examined this strong influence of river inflow on circulation and in turn on the silica concentrations by assuming simple distributions of silica uptake by phytoplankton production. The silica concentrations are primarily controlled by rates of river supply, biological removal, and dilution with seawater.

### **The real system: circulation, phytoplankton and silica**

During much of the year the northern Bay is a partially mixed estuary with its circulation and salinity responding to variations in river inflow. During winter, salt water intrudes landward to San Pablo Bay and in summer to Rio Vista (Figure 1). The salt field probably never fully achieves steady-state adjustment with the water circulation even after a period of weeks of near-uniform river inflow. The salinity is generally low in relation to river inflow during summer and may be high during winter because of the lag in response of salinity to discharge (Ward & Fischer, 1971).

The few current-meter surveys in the main channel suggest that the null zone (where river and density currents are equal and opposite) is located about 20 km from the seaward end of the estuary (Golden Gate) when river discharge is  $2000 \text{ m}^3 \text{ s}^{-1}$  and 80 km when it is  $100 \text{ m}^3 \text{ s}^{-1}$  (Peterson *et al.*, 1975b). The corresponding distances of salinity penetration are 40 and 90 km from the seaward end.

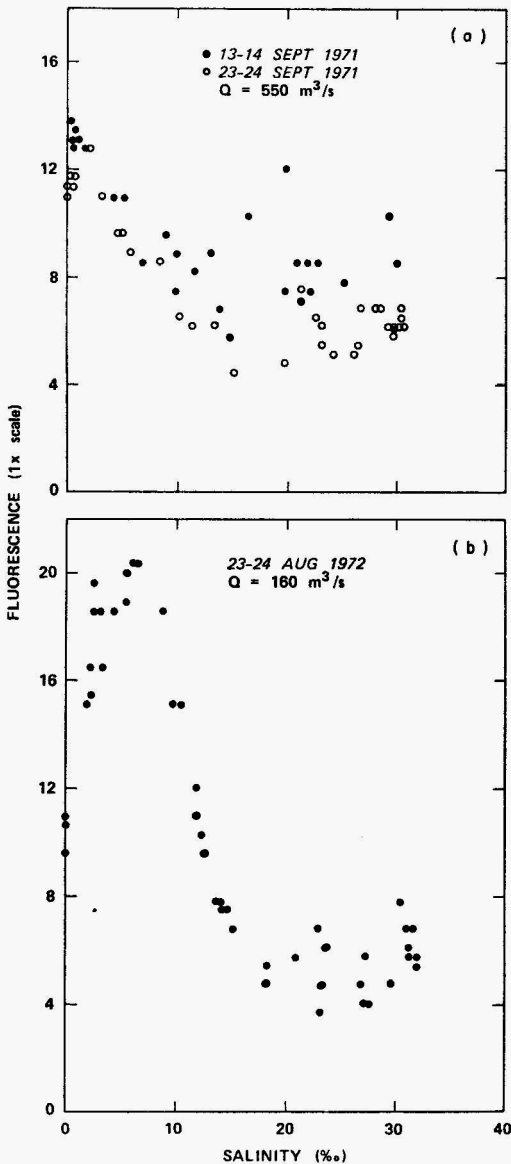


Figure 2. Longitudinal covariance of *in vivo* chlorophyll *a* with salinity (2-m depth) at different river inflows. Chlorophyll *a* measured with Turner fluorometer and expressed as fluorescence units.  $Q$  is combined mean monthly inflows of the Sacramento and San Joaquin rivers.

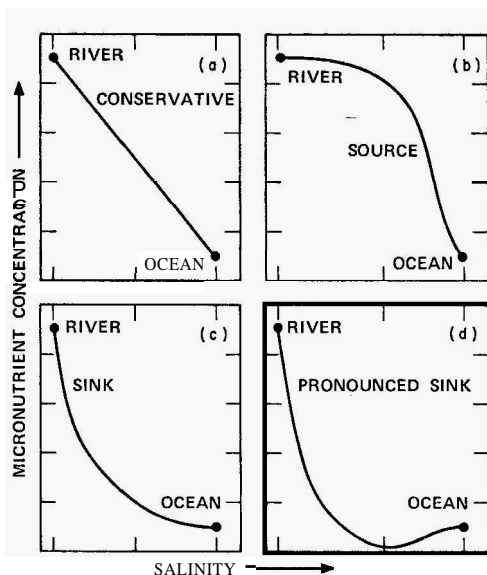


Figure 3. Idealized longitudinal distributions of salinity covarying with a non-conservative substance which has a higher concentration in river water than seawater. (a) Horizontal mixing rates dominate and effects of internal sources or sinks are negligible; (b) secondary source is present; (c) sink is present; (d) sink is pronounced relative to the horizontal mixing rate. After Peterson et al. (1975a).

Winter river inflows are typically above  $400\text{--}500\text{ m}^3\text{ s}^{-1}$ ; summer inflows are lower. During winter the phytoplankton distribution (as indicated by chlorophyll *a* measurements) is relatively uniform, whereas during summer the phytoplankton levels may increase in the upper estuary (phytoplankton maximum), particularly during lower-than-normal inflows (Figure 2). Phytoplankton productivity per unit volume is often highest in the phytoplankton maximum (Conomos & Peterson, 1974). Based on a unit area, however, productivity may be lower in the phytoplankton maximum than in a seaward direction where the euphotic zone is deeper (cf., Williams, 1966; Flemer, 1970). Diatoms are usually the most abundant phytoplankton, and increases in chlorophyll parallel increases in silica uptake.

The influence of nonconservative processes on the distribution of reactive substances is probably best demonstrated by relating the substances, such as silica, to salinity. In the Bay, silica-salinity distributions are represented by three [Figure 3(a), (c) and (d)] of four simple examples, with internal silica sources negligible [Figure 3(b)]. This is not always the case; in the Hudson River estuary, for example, internal silica sources (sewage) are excessive (Simpson et al., 1975).

The seasonal silica-salinity variations are not steady-state distributions (Peterson et al., 1975a). All data indicate that it takes weeks to depress silica to low concentrations from near-linear values. During summer, silica departs from near-linear values with salinity at river inflows less than  $400\text{--}500\text{ m}^3\text{ s}^{-1}$  (Figure 4) and is depressed the most during the lowest inflows of less than  $100\text{ m}^3\text{ s}^{-1}$ .

Although silica uptake by phytoplankton is a depth-dependent process (unpublished data), differences in silica-salinity distributions have not been observed between surface and bottom waters (Figure 5). Effects of depth-variable silica uptake are apparently reduced or eliminated by vertical mixing.

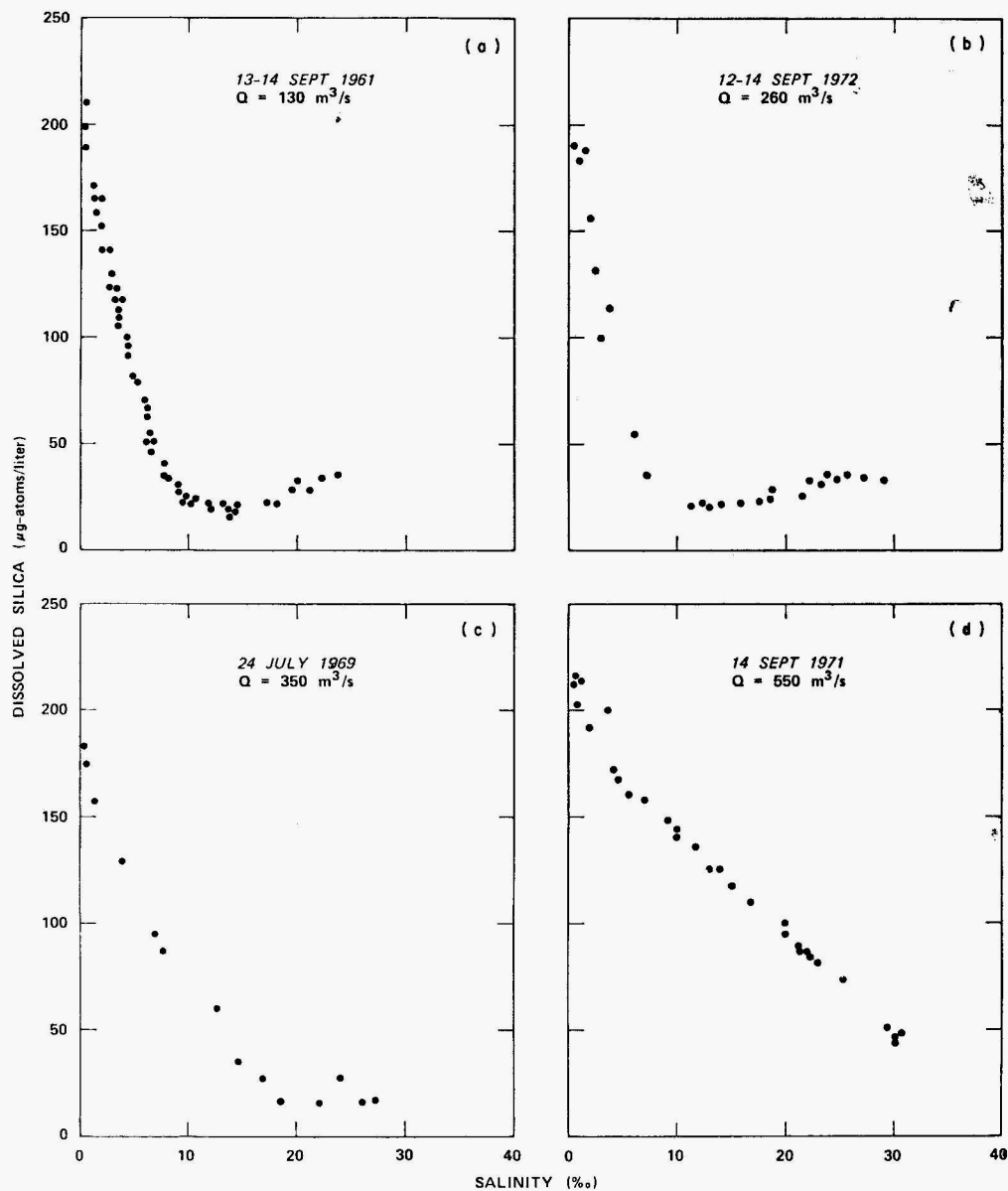


Figure 4. Observed silica-salinity covariance (2-m depth) for different mean monthly river inflows ( $Q$ ). Data in (a) are from McCarty *et al.* (1962).

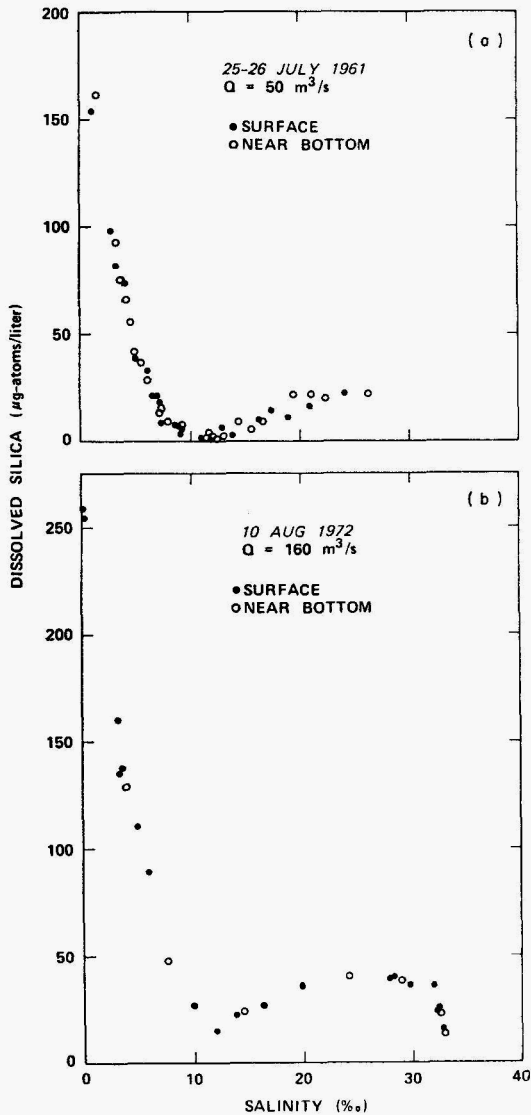


Figure 5. Observed silica-salinity covariance in surface (1-m depth) and bottom waters during periods of maximum biological removal. Data in (a) are from McCarty *et al.* (1962).  $Q$  is mean monthly river inflow.

### The numerical silica model

Because of the lack of field data, the dynamics of San Francisco Bay estuary are defined using the numerical model of Festa & Hansen (1976) which describes a two-dimensional, steady-state, gravitational circulation. The depth and width of the estuary are assumed constant, as are the mixing coefficients of salt and momentum. This circulation model is especially advantageous for our needs because it describes the dynamics of the transition from river to estuary and the variations in dynamics with river inflow.

Development of our silica model is consistent with the Festa-Hansen description of

circulation in partially mixed estuaries (Festa & Hansen, 1976). The governing equation for the silica concentration is:

$$\frac{\partial Si}{\partial t} + uSi_x + wSi_z = K_h Si_{xx} + K_v Si_{zz} - \text{uptake}, \quad (1)$$

where  $Si$  is the silica concentration ( $\text{pg-at. l}^{-1}$ );  $u$  and  $w$  are the horizontal and vertical components, respectively, of tidally averaged velocity;  $K_h$  and  $K_v$  are the horizontal and vertical exchange coefficients of silica and represent a measure of the strength of tidal mixing; and 'uptake' is the parametric representation of the silica utilization rate by phytoplankton production ( $\text{pg-at. l}^{-1} \text{ day}^{-1}$ ).

Representative boundary values for silica are:

$$\begin{aligned} Si(x = \text{ocean}, z = 10 \text{ m}) &= 30 \text{ pg-at. l}^{-1}; \\ Si(x = \text{river}) &= 200 \text{ pg-at. l}^{-1}. \end{aligned}$$

The depth,  $H$ , is specified at 10 m and represents a typical value of the main channel where velocity, salinity, and silica data have been collected (Figure 1). The finite-difference techniques used to model silica are exactly the same as those developed for the circulation field.

Effects of the riverflow, silica-uptake rates, and vertical exchange coefficients on silica distributions were considered. River inflows of 100, 200, 400 and 2000  $\text{m}^3 \text{s}^{-1}$  were simulated by approximating river currents of 1, 2, 4 and 20  $\text{cm s}^{-1}$  at the river boundary. The first three inflow rates represent typical low, intermediate, and high summer river levels. The last, 2000  $\text{m}^3 \text{s}^{-1}$ , is a typical high winter rate. Bottom water salinity at the ocean boundary of 30‰ was specified in all cases, except for a value of 25‰ at 2000  $\text{m}^3 \text{s}^{-1}$ . Silica-uptake rates and vertical exchange coefficients, which were varied, are discussed in the following section.

We first approximated the water-circulation and salinity-diffusion processes using the Festa-Hansen model, and then applied this field to the silica model. The general circulation of Bay waters (Conomos, 1975) and some of its variations with river inflow (Peterson *et al.*, 1975b) provided an approximation for evaluating the response of the Festa-Hansen model to river inflow as well as a basis for estimating the mixing coefficients. No attempt was made to adjust closely the Festa-Hansen model to various field conditions because of simplifications in the numerical model and our limited knowledge of the real circulation. Our major concern is to produce a reasonable approximation of gravitational circulation for various river inflows, as this circulation drives the flow in our silica model.

### The numerical simulation

Vertical velocity and salinity distributions generated by the Festa-Hansen circulation model are presented for river inflows of 100, 200, 400 and 2000  $\text{m}^3 \text{s}^{-1}$  (Figure 6). The seaward movement of the null zone with increasing inflow is similar to results obtained from the few available current-meter observations. The response of water circulation and salinity to variations in vertical exchange of salt ( $K_v$ ) and momentum ( $A_v$ ) is also examined (Figure 7). The model indicates that increasing vertical exchange of momentum weakens estuarine circulation, and that increasing vertical exchange of salt strengthens the circulation.

The circulation and salinity fields obtained using the vertical exchange Coefficients of  $A_v = 20 \text{ cm}^2 \text{s}^{-1}$  and  $K_v = 4 \text{ cm}^2 \text{s}^{-1}$  give a reasonable approximation to field conditions, and were thus used to generate the dynamics for the silica model.

Effects of river inflow on silica distributions were examined using two hypothetical cases for silica uptake: (1) Constant and vertically uniform uptake throughout the estuary (Figure 8),

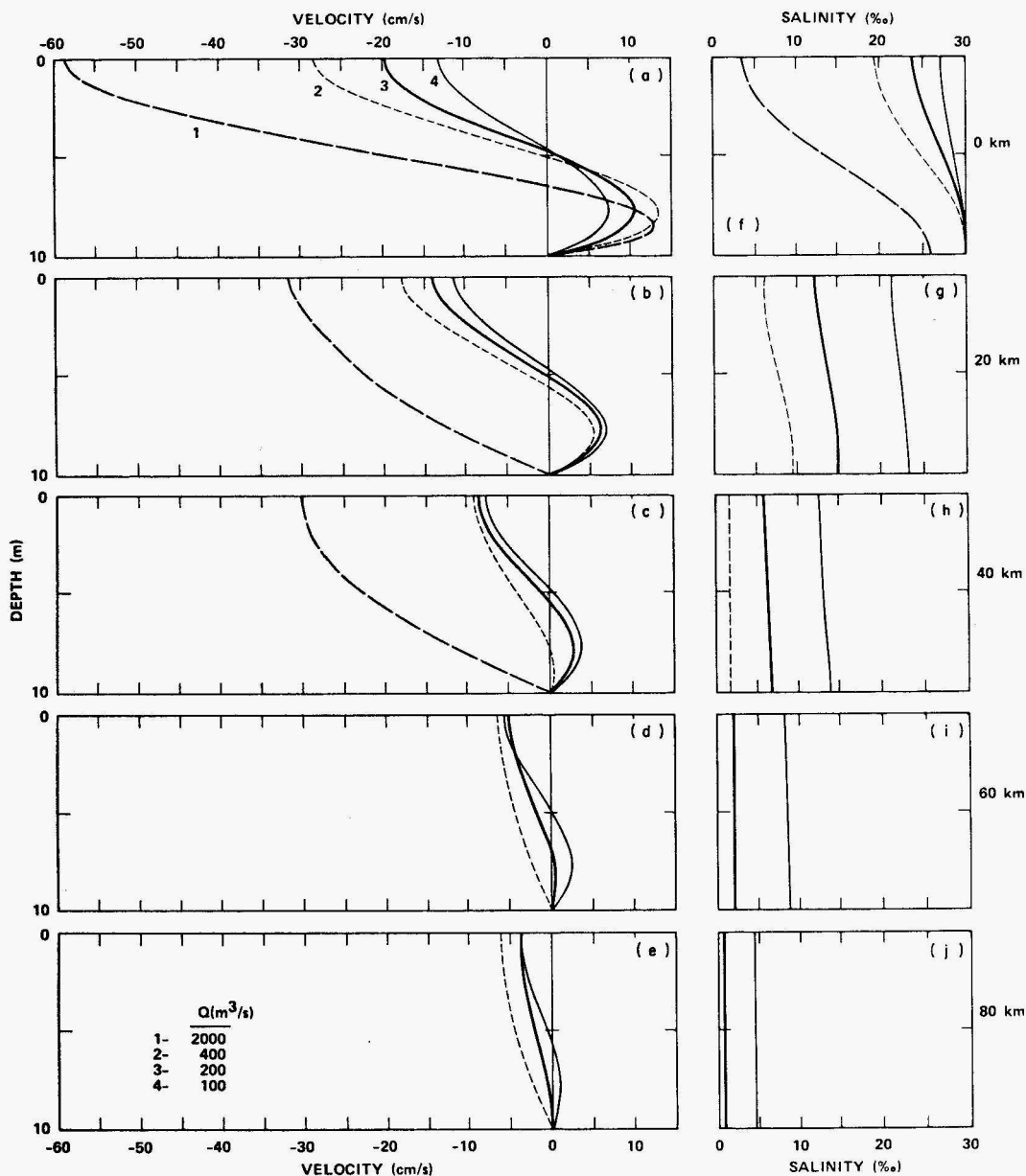


Figure 6. Simulated longitudinal variations of velocity and salinity for various river inflows ( $Q$ ) at several locations in the estuary. Computational length for river currents of 1, 2, 4, and 30  $\text{cm s}^{-1}$  are 160, 120, 64 and 48 km respectively. The horizontal mixing coefficients of salt ( $K_h$ ) and momentum ( $A_h$ ) were specified at  $4 \times 10^8$  and  $10^7 \text{ cm}^2 \text{ s}^{-1}$ , respectively; the vertical mixing coefficients are  $K_v = 4$  and  $A_v = 10 \text{ cm}^2 \text{ s}^{-1}$ , respectively.



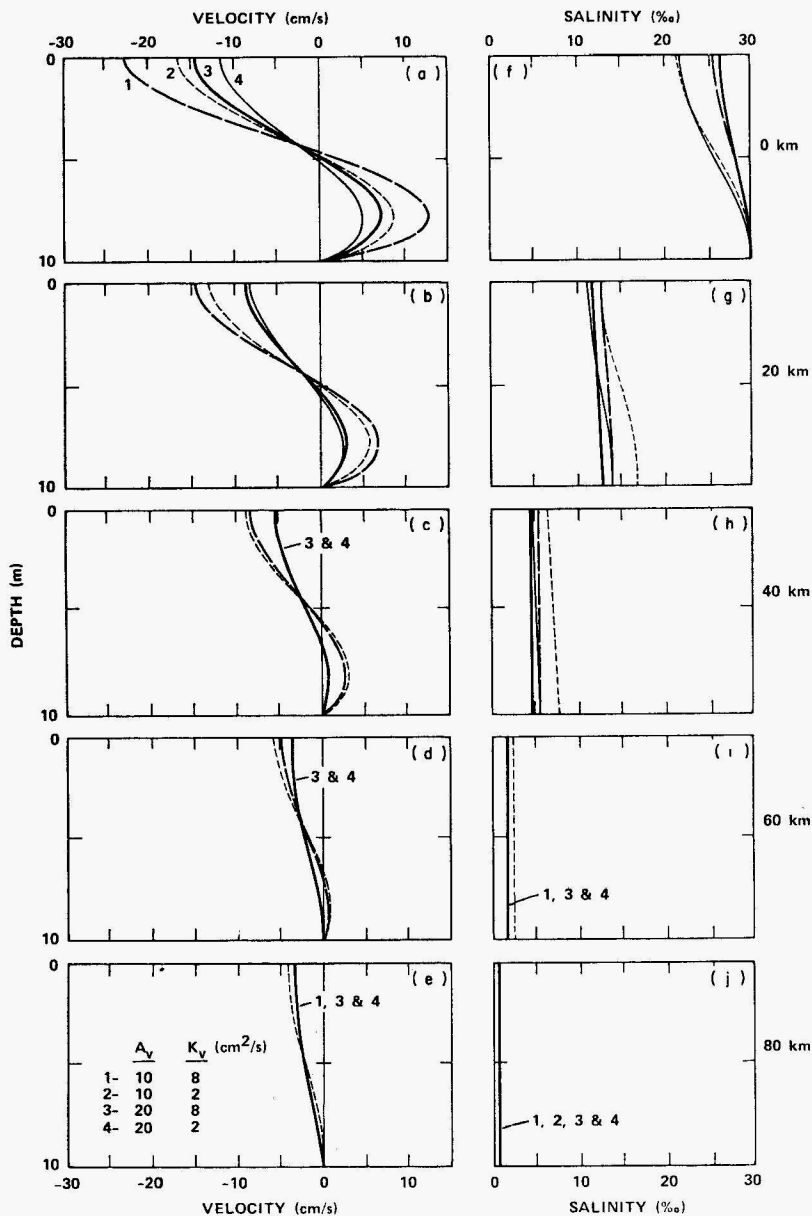


Figure 7. Simulated longitudinal variations of velocity and salinity for various vertical mixing coefficients of salt ( $K_v$ ) and momentum ( $A_v$ ) at different locations in the estuary. The river current is constant at  $2 \text{ cm s}^{-1}$ .  $K_h = 4 \times 10^6$  and  $A_h = 10^7 \text{ cm}^2 \text{ s}^{-1}$ .

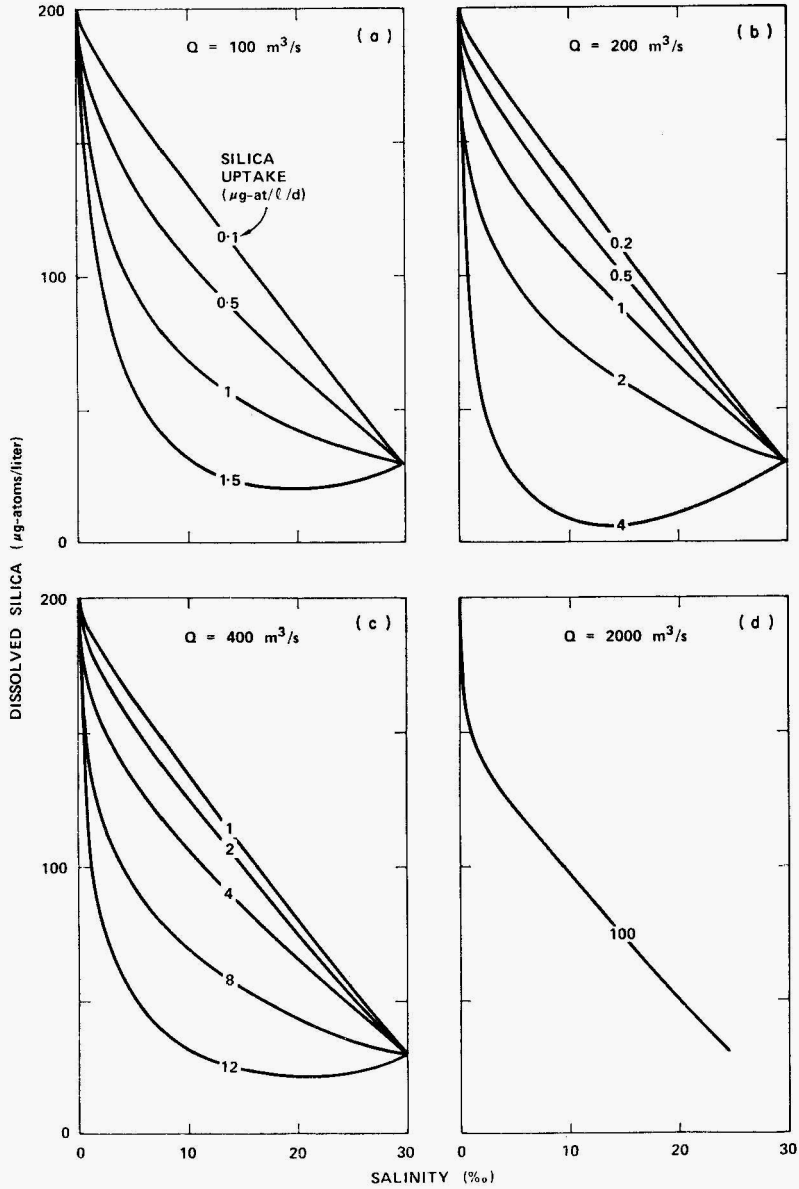


Figure 8. Simulated silica-salinity covariance for different river inflow ( $Q$ ) and silica uptake rates.  $K_v = 4$  and  $A_v = 20 \text{ cm}^2 \text{ s}^{-1}$ ;  $K_h = 4 \times 10^6$  and  $A_h = 10^7 \text{ cm}^2 \text{ s}^{-1}$ . Silica uptake for each simulation is vertically uniform throughout the estuary.

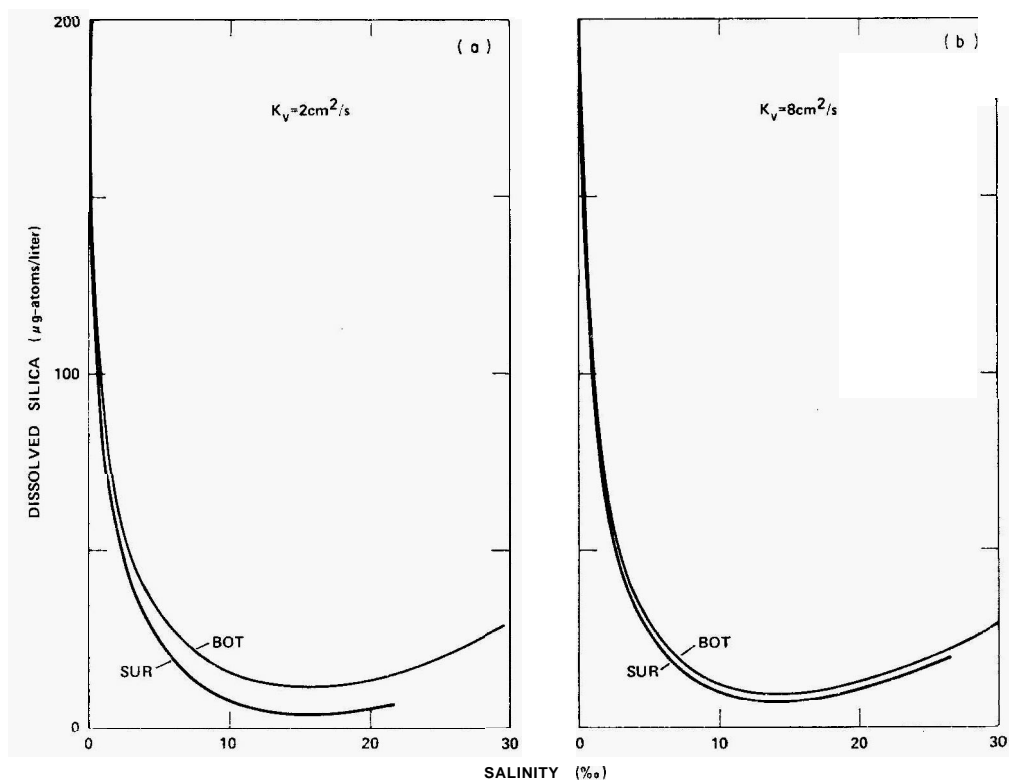


Figure 9. Simulated silica-salinity covariance in surface (SUR) and bottom (BOT) waters as a function of varying vertical salt (and silica) mixing coefficients ( $K_v$ ). A, is  $20 \text{ cm}^2 \text{ s}^{-1}$ , and the river current is  $2 \text{ cm s}^{-1}$ . Silica uptake is  $12 \text{ pg-at. l}^{-1} \text{ day}^{-1}$  in upper  $2.5 \text{ m}$  and zero below that depth.

and (2) constant uptake in the upper few meters and zero uptake below (Figure 9). The latter seems more realistic since uptake rates are near zero below the euphotic zone. In both cases the conservative effects of water advection and diffusion were initially simulated for zero silica uptake throughout the estuary. Solutions were then obtained for relatively small utilization rates, and were gradually increased until the minimum silica concentrations approached the growth-rate limiting concentrations of 4 to  $12 \text{ pg-at. l}^{-1}$  (Paasche, 1973a, b; Davis *et al.*, 1973; Harrison, 1974; Goering *et al.*, 1973), and for completeness, an unrealistically large value of  $100 \text{ pg-at. l}^{-1} \text{ day}^{-1}$  [Figure 8(d)]. Limiting maximum uptake rates in this fashion eliminated the complication of introducing utilization terms which depend on silica.

Results from constant silica uptake throughout the estuary show that  $1.5 \text{ pg-at. l}^{-1} \text{ day}^{-1}$  ( $15 \text{ mg-at. m}^{-2} \text{ day}^{-1}$ ) is sufficient to depress strongly silica concentrations at an inflow of  $100 \text{ m}^3 \text{ s}^{-1}$  [Figure 8(a)]. This rate has only a moderate effect on the silica-salinity distribution at  $200 \text{ m}^3 \text{ s}^{-1}$  [Figure 8(b)] and produces only a minor departure from a linear (conservative) distribution at  $400 \text{ m}^3 \text{ s}^{-1}$  [Figure 8(c)].

Silica-salinity distributions obtained from constant uptake in the upper  $2.5 \text{ m}$  and zero below (Figure 9) are similar to those assuming constant and vertically uniform uptake

throughout the estuary (Figure 8). In this formulation, however, the utilization rates must be 4 times higher since they are applied to only one-fourth the water depth.

Depth variations of observed silica-salinity distributions are on the order of a few  $\mu\text{g-at. l}^{-1}$ , the equivalent of the observed variability (Figures 4 and 5). Such variations are approached for simulations in which the vertical exchange coefficient,  $K_v$ , is  $8 \text{ cm}^2 \text{ s}^{-1}$  [Figure 9(b)]. This coefficient, which also gives reasonable circulation fields, results in a silica diffusive time scale,  $H^2/K_v$ , of approximately 1.4 days, and indicates that surface water of the euphotic zone may be mixed over the entire water column in nearly 1 day.

### Conservative versus nonconservative processes

Our immediate interest in modelling silica was to estimate rates of biological removal at which silica behaves conservatively and nonconservatively for various river inflows, and thus, to determine under what conditions physical processes maintain near-linear silica-salinity distributions. Water circulation and uniform biological uptake of silica are considered as two independent but competing processes. Estuarine silica-salinity distributions would either remain linear, vary seasonally or remain non-linear and should depend on the relative strengths of these processes. Model results indicate utilization rates necessary to produce three of these possibilities [Figure 8(a), (b) and (c)].

Field observations illustrate a seasonal variation in silica-salinity concentrations (Figure 4). Although depression of silica concentrations is a common occurrence during low summer inflow, such depression has never been observed in over 10 years of near-monthly surveys at inflows greater than  $400 \text{ m}^3 \text{ s}^{-1}$ .

If the silica uptake rates required to produce a marked non-linear silica-salinity distribution are unrealistic, it would explain why the natural conditions remain near-linear at discharges greater than  $400 \text{ m}^3 \text{ s}^{-1}$ . If we assume an inflow of  $400 \text{ m}^3 \text{ s}^{-1}$ , a 10-m water column, and a 1-m euphotic zone (the field conditions of the phytoplankton-turbidity maximum), uptake in the upper meter must approach  $120 \text{ pg-at. Si l}^{-1} \text{ day}^{-1}$  to depress strongly the silica concentrations. Phytoplankton productivity would be more than  $5000 \text{ mg C m}^3 \text{ day}^{-1}$ , assuming a (moderate) Si : C ratio of 1 : 4. Limited field observations (unpublished) indicate that this production rate is an order of magnitude too high. Thus the model provides an estimate of average silica utilization rates ( $1\text{--}10 \text{ pg-at. l}^{-1} \text{ day}^{-1}$ ) which are roughly equivalent to that from other methods (e.g., carbon productivity).

### Residence time

Water residence time, the average time required for water to enter and leave the estuary, is influenced by both advective and diffusive processes. River inflow and density currents control advective processes, while wind and tidal mixing control diffusive processes. Wind is omitted in the following discussion.

In general, river currents decrease in the seaward direction with increasing cross-channel area, whereas inward flowing density currents ultimately weaken to equal the opposing river current (null zone); tidal mixing attenuates landward. The net effect of these processes may produce a longitudinal variation in the advective and diffusive replacement time of a substance (Figure 10).

As the river flow increases the null zone shifts seaward and the residence time decreases. Average bottom density currents seldom exceed  $15 \text{ cm s}^{-1}$  and do not increase dramatically with increasing river inflow (Officer, 1976). It follows that as river currents increase to 10

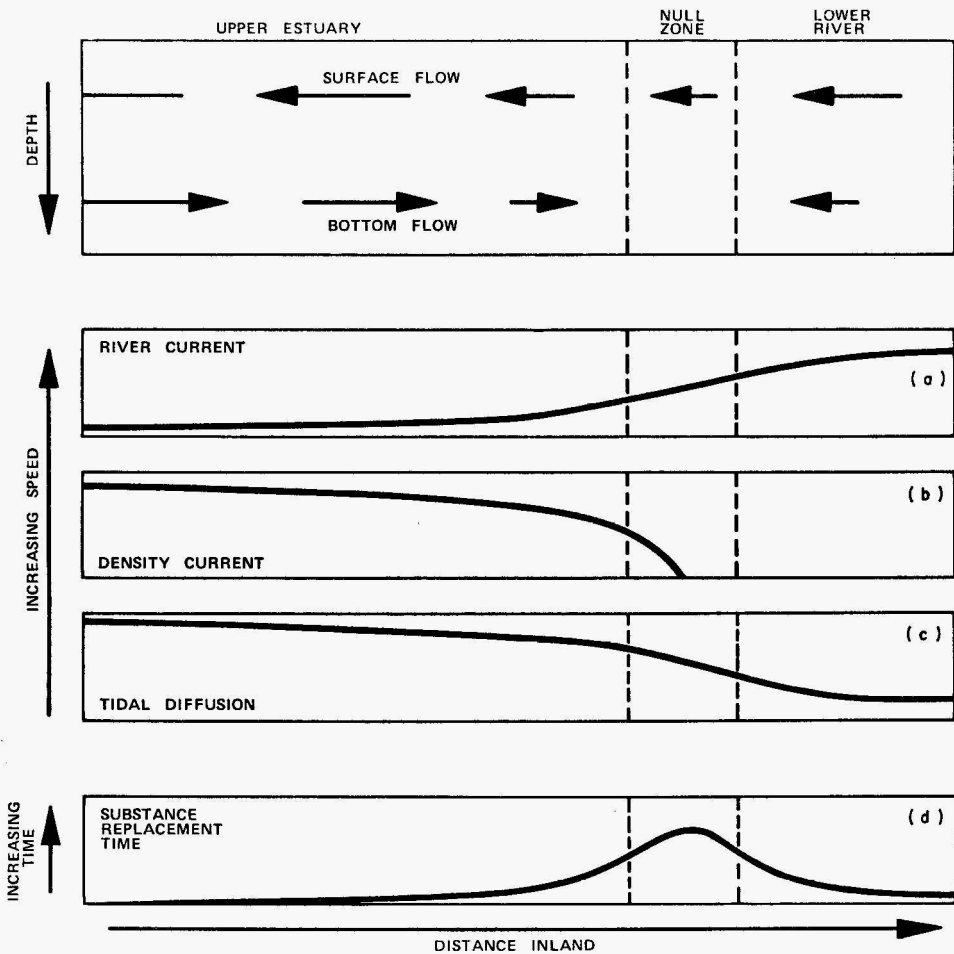


Figure 10. Qualitative contributions of river current (a), density current (b), and tidal diffusion (c) to longitudinal variations in substance replacement time (d) in a hypothetical estuary. Modified after Peterson *et al.* (1975a).

$\text{cm s}^{-1}$ , longitudinal variations in advective water replacement time may be relatively small.

Model results (Figures 8, 9) indicate that higher phytoplankton productivity in the null zone is not essential for development of the observed silica salinity distribution. It is possible that even with lower rates of silica uptake, silica concentrations are still strongly depressed in the null zone. Such effects can be produced by an increased water and particle (phytoplankton) residence time in the inner estuary: a column of water there may not necessarily receive more sunlight per unit time than in the outer estuary, but the water (and phytoplankton) may receive sunlight over a longer time.

Advective water-replacement time per unit width and length are estimated from the 10-m depth model:

$$\bar{V}_{\text{river inflow}(r_l)} = \frac{1}{10} \int_0^{10} V(z)_{r_l} dz \quad (2)$$

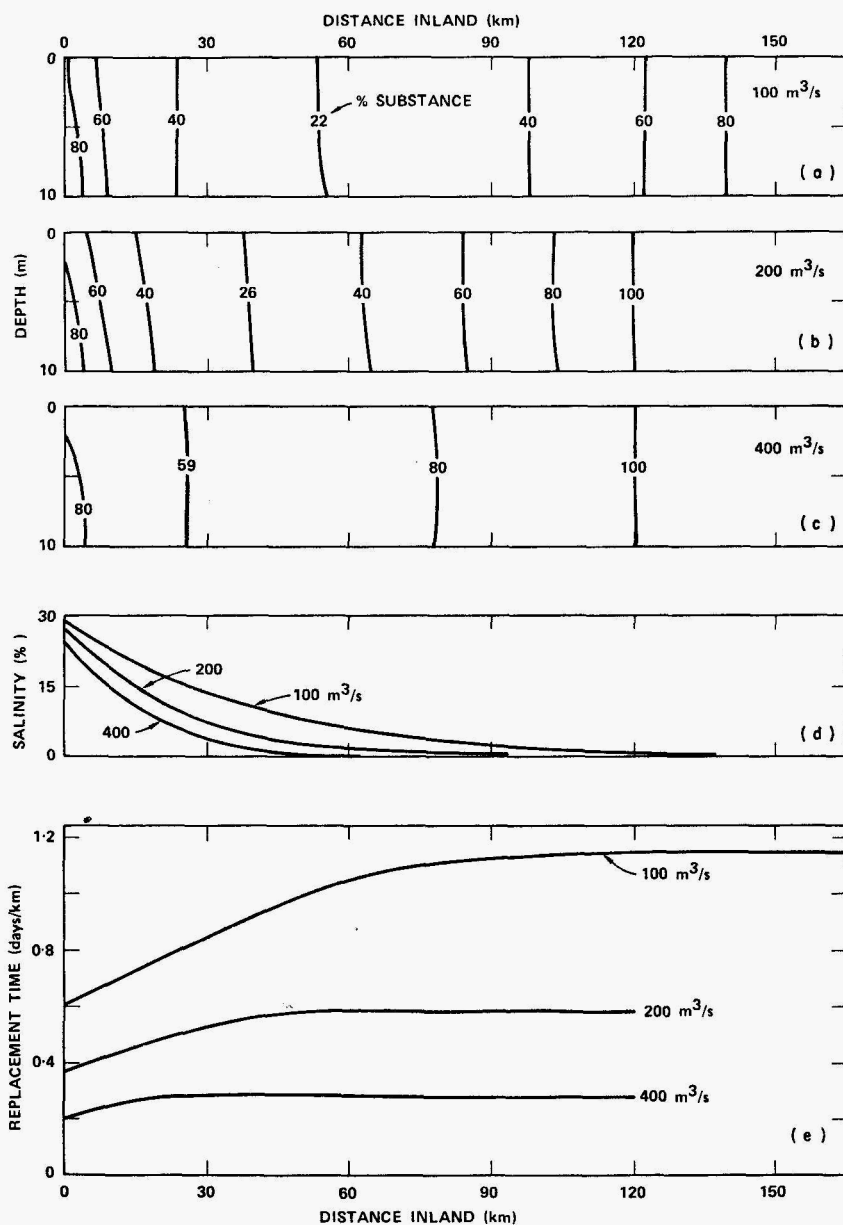


Figure 11. Simulated distribution of a nonconservative substance (per cent present) with distance as functions of various river inflows (a, b, c) assuming 100% input of substance at both river and ocean boundaries and a continuous uptake of  $1\%$   $\text{day}^{-1}$  for  $100 \text{ m}^3 \text{ s}^{-1}$  and  $2\%$   $\text{day}^{-1}$  for 200 and  $400 \text{ m}^3 \text{ s}^{-1}$ . (d) Simulated salinity distribution at 5 m at various river inflows. (e) Simulated nonconservative substance replacement time for averaged water column as a function of distance at various river inflows.  $K_v = 4$  and  $A_v = 20 \text{ cm}^2 \text{ s}^{-1}$ .

$$\bar{V}_{\text{ocean inflow}(oi)} = \frac{1}{10} \int_0^z, \text{ where } V_{oi} = 0 \quad V(z)_{oi} dz \quad (3)$$

$$\text{and replacement time} = \frac{\text{Length}}{\bar{V}_{ri} + \bar{V}_{oi}} \quad (4)$$

where  $\bar{V}$  is the mean current speed. Note that because the model represents constant width, maximum water-replacement time is in the river [Figure 11(e)].

Advective water-replacement times per unit width, for a 120-km river-estuary system, are estimated from the model to be 75, 45 and 25 days for river inflows of 100, 200 and 400  $\text{m}^3 \text{s}^{-1}$  respectively ( $A_v = 20 \text{ cm}^2 \text{s}^{-1}$ ;  $K_v = 4 \text{ cm}^2 \text{s}^{-1}$ ). In these time periods, on the average, a conservative substance introduced continuously at the center of the 120-km system may move by eddy diffusivity ( $K_h = 4 \times 10^6 \text{ cm}^2 \text{s}^{-1}$ ) about 70, 55 and 40 km, respectively ( $\sqrt{2K_h T}$ ).

The silica model can be used to illustrate effects of advective and diffusive processes on substance replacement time by maintaining 100 units of silica at both river and ocean boundaries. Note the seaward shift in minimum concentration with increasing river inflow [Figure 11(a), (b) and (c)]. In a typical simulation, the minimum (steady-state) concentration was about 26 units in the null zone for a river discharge of 200  $\text{m}^3 \text{s}^{-1}$  and a uniform uptake rate of 2 units per day. We can estimate that it takes  $(100 - 26)/2$  units per day, or a 37-day maximum silica-replacement time, to produce this distribution (Figure 12). Because diffusive processes are included, this is less than the advective replacement time estimated above.

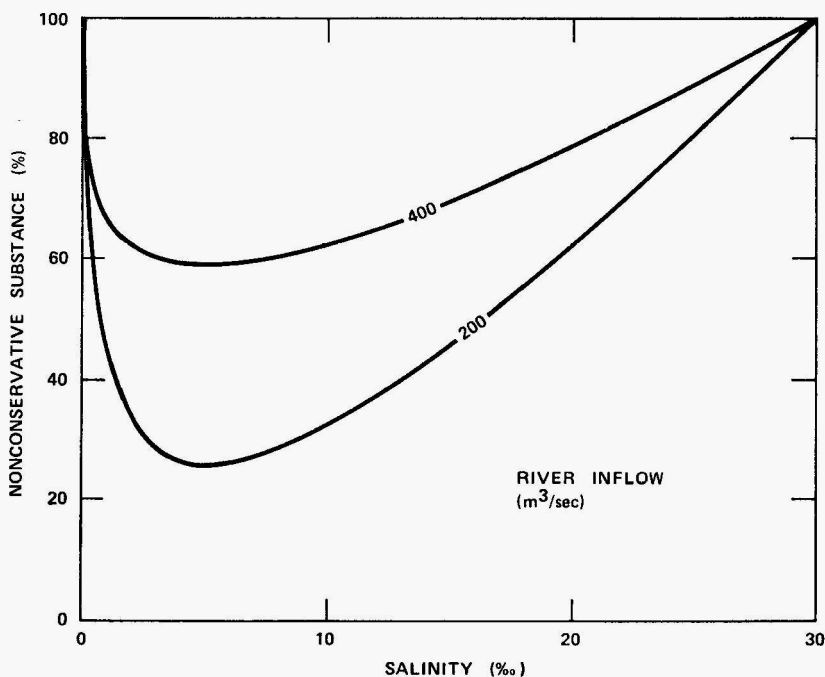


Figure 12. Simulated distribution of a nonconservative substance with salinity as a function of various river inflows assuming 100% input of substance at both river and ocean boundaries and a constant uptake of 2% per day.  $K_v = 4$  and  $A_v = 20 \text{ cm}^2 \text{s}^{-1}$ .

The combination of an uptake of 1 unit per day and a river discharge of  $100 \text{ m}^3 \text{ s}^{-1}$  has a silica distribution similar to the  $200 \text{ m}^3 \text{ s}^{-1}$  example, and indicates an 80-day maximum silica replacement time for a 160-km system.

Average rates of silica utilization can be estimated using the above results. For example, the maximum departure of silica concentrations from a conservative distribution is about  $125 \mu\text{g-at. l}^{-1}$  at  $130 \text{ m}^3 \text{ s}^{-1}$  [Figure 4(a)]. If the water residence time is approximately 60 days at this inflow, estimated silica uptake is  $2 \mu\text{g-at. l}^{-1} \text{ day}^{-1}$ . The silica-salinity distribution in Figure 4(b) is essentially identical to Figure 4(a) but inflow is twice as high, giving an average uptake of about  $4 \mu\text{g-at. l}^{-1} \text{ day}^{-1}$ . These are gross estimates because the field data are not true steady state distributions. As such, the silica-salinity distribution measured at  $260 \text{ m}^3 \text{ s}^{-1}$  may be influenced by the lower ( $160 \text{ m}^3 \text{ s}^{-1}$ ) inflow of the preceding month producing a lower estimated utilization rate. It may also be difficult to estimate total inflow, especially during low summer flows when the amount of water consumption by agricultural activities downstream of river gauging sites is appreciable and not clearly determined.

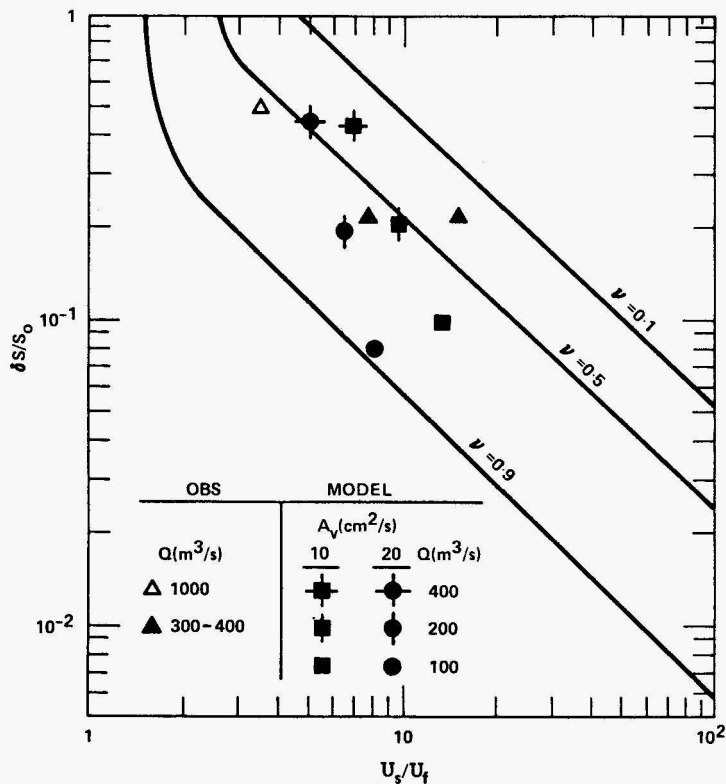


Figure 13. Observed and simulated fractions ( $v$ ) of horizontal salt balance by diffusion as functions of salinity stratification ( $\delta S/S_0$ ) and estuarine circulation ( $U_e/U_r$ ). Values from numerical simulation (MODEL) represent circulation at the seaward boundary. Observed data (OBS), from Peterson & Conomos (1975) and were collected at Carquinez Strait (Figure 1). Note variation with increased river inflow ( $Q$ ) and with increased vertical mixing coefficients of momentum ( $A_v$ ). Diagram from Hansen & Rattray (1966).



### Advective and diffusive processes

Knowledge of the relative strengths of advective and diffusive processes is helpful in understanding the development of non-conservative silica distributions in estuaries. The Hansen-Rattray (1966) estuarine classification diagram provides an estimate of the relative contribution of either process toward landward salt transport and is especially appropriate for describing results from the Festa-Hansen circulation model (Figure 13).

For illustrative purposes, we selected the model circulation-salinity values from its seaward boundary (and the few field observations at Carquinez Strait, Figure 1). Increasing river inflow shifts these values diagonally toward the upper left of the diagram with an associated decrease in water replacement time.

This diagram can characterize the circulation when silica behaves conservatively. Obviously, a field in the diagram of increased river inflow (upper left) is a regime of linear or near-linear silica-salinity distributions as long as the silica utilization rate giving conservative distributions at lower inflow does not increase. Hence, silica may always appear conservative during 'high' inflow. It is interesting that linear silica-salinity distributions may typify most temperate estuaries (Fanning & Pilson, 1973; Boyle *et al.*, 1974); unfortunately, their position on the Hansen-Rattray diagram is usually undefined.

### A hypothetical season

We summarize the effects of estuarine dynamics on silica distributions by describing a typical spring to fall sequence of river inflow.

During late spring, inflow decreases to approximately  $400\text{--}500\text{ m}^3\text{ s}^{-1}$  and insolation increases. The longitudinal distribution of phytoplankton is uniform. A larger portion of the estuary is influenced by the density currents, as is shown by increased salt penetration and by landward movement of the null zone. The maximum replacement time is approximately 20 days and silica uptake rates (averaged over the water column) are between 1 and 2 pg-at.  $l^{-1}\text{ day}^{-1}$ . Silica-salinity distributions remain conservative (near-linear) at these utilization rates, since it takes more than 20 days to depress silica strongly.

Inflow continues to decrease during summer, while phytoplankton increases in abundance particularly in the upper estuary. Rates of silica uptake may increase slightly. More significantly, however, the river supply rate of silica decreases and water residence time increases. At an inflow of  $200\text{ m}^3\text{ s}^{-1}$ , the replacement time is about 40 days. Silica concentrations become depressed in approximately one month, producing non-conservative distributions. If inflow decreases to  $100\text{ m}^3\text{ s}^{-1}$  a conspicuous phytoplankton maximum persists in the upper estuary where the non-tidal currents are weak, and average silica uptake rates may exceed 1 to 2 pg-at.  $l^{-1}\text{ day}^{-1}$ . Replacement time is more than 70 days; silica concentrations are well below 70 pg-at.  $l^{-1}$  from their predicted conservative concentrations and may approach growth-rate limiting levels.

Inflow increases during fall, silica input exceeds removal by phytoplankton, and eventually silica-salinity distributions become conservative (linear).

This scenario is illustrated by all years for which there are silica data (1961–64 and 1968–present) with the exception of 1976, an unusually dry year during which silica remained near-linear during low inflow. Such 'anomalous' behavior is currently under investigation.

## Acknowledgements

We thank W. W. Broenkow, D. E. Hammond, D. V. Hansen and C. B. Officer for helpful discussions and criticisms.

## References

- Boyle, E., Collier, R., Dengler, A. T., Edmond, J. M., Ng, A. G. & Stallard, R. F. 1975 On the chemical mass-balance in estuaries. *Geochimica et Cosmochimica Acta* 38, 1719-1728.
- Conomos, T. J. 1975 Movement of spilled oil as predicted by estuarine nontidal drift. *Limnology and Oceanography* 20, 159-173.
- Conomos, T. J. & Peterson, D. H. 1974 Biological and chemical aspects of the San Francisco Bay turbidity maximum. *Memoirs de l'Institut de Géologie du Bassin d'Aquitaine* 7, 45-52.
- Conomos, T. J. & Peterson, D. H. 1976 Suspended-particle transport and circulation in San Francisco Bay: an overview. *Proceedings of the 3rd Meeting of the International Estuarine Research Federation Conference* (in press).
- Davis, C. O., Harrison, P. J. & Dugdale, R. C. 1973 Continuous culture of marine diatoms under silicate limitation. I. Synchronized life cycle of *Skeletonema costatum*. *Journal of Phycology* 9, 175-180.
- Dyer, K. R. (in press) Lateral effects in estuaries. *Symposium on Estuaries, Geophysics, and the Environment*. AAAS Meetings, 1976.
- Fanning, K. A. & Pilson, M. E. Q. 1973 The lack of inorganic removal of dissolved silica during river-ocean mixing. *Geochimica et Cosmochimica Acta* 37, 2405-2415.
- Festa, J. F. & Hansen, D. V. 1976 A two-dimensional commercial model of estuarine circulation: the effects of altering depth and river discharge. *Estuarine and Coastal Marine Science* 4, 309-323.
- Flemer, D. A. 1970 Primary production in the Chesapeake Bay. *Chesapeake Science* 11, 117-129.
- Goering, J. J., Nelson, D. M. & Carter, J. A. 1973 Silicic acid uptake by natural populations of marine phytoplankton. *Deep-Sea Research* 20, 777-789.
- Hansen, D. V. & Rattray, M. Jr. 1966 New dimensions in estuary classification. *Limnology and Oceanography* 11, 319-326.
- Harrison, P. J. 1974 Continuous culture of the marine diatom *Skeletonema costatum* (Grev.) Cleve under silicate limitation. Ph.D. thesis, Univ. Washington, Seattle, 140 pp.
- McCarty, J. C., Wagner, R. A., Macomber, M., Harris, H. S., Stephenson, M. & Pearson, E. A. 1962 An investigation of water and sediment quality and pollutional characteristics of three areas in San Francisco Bay 1960-61. Sanitary Engineering Research Laboratory, University of California, Berkeley, California. 571 pp.
- Officer, C. B. (in press) Longitudinal circulation and mixing relations in estuaries. *Symposium on Estuaries, Geophysics, and the Environment*. AAAS Meetings, 1976.
- Paasche, E. 1973a Silicon and the ecology of marine plankton diatoms. I. *Thalassiosira pseudonana* (*Cyclotella nana*) grown in a chemostat with silicate as limiting nutrient. *Marine Biology* 19, 117-126.
- Paasche, E. 1973b Silicon and the ecology of marine plankton diatoms. II. Silicate-uptake kinetics in five diatom species. *Marine Biology* 19, 262-269.
- Peterson, D. H., Conomos, T. J., Broenkow, W. W. & Scrivani, E. P. 1975a Processes controlling the dissolved silica distribution in San Francisco Bay. In *Estuarine Research—Chemistry and Biology* (Cronin, L. E., ed.). Academic Press, London and New York, Vol. 1, pp. 153-187.
- Peterson, D. H., Conomos, T. J., Broenkow, W. W. & Doherty, P. C. 1975b Location of the nontidal current null zone in northern San Francisco Bay. *Estuarine and Coastal Marine Science* 3, 1-11.
- Peterson, D. H. & Conomos, T. J. 1975 Implications of seasonal chemical and physical factors on the production of phytoplankton in northern San Francisco Bay. In *Proceedings of the Workshop on Algal-Nutrient Relationships in the San Francisco Bay and Delta*. (Brown, R. L., ed.). The San Francisco Bay and Estuarine Association. pp. 147-165.
- Simpson, H. J., Hammond, D. H., Deck, B. L. & Williams, S. C. 1975 Nutrient budgets in the Hudson River Estuary. In *Marine Chemistry in the Coastal Environment*. (Church, T. M., ed.). A.C.S. Symposium Series, No. 18, pp. 618-635. 710pp.
- Ward, R. B. & Fischer, H. B. 1971 Some limitations on use of the one-dimensional dispersion equation, with comments on two papers by R. W. Paulson. *Water Resources Research* 7, 215-220.
- Williams, R. B. 1966 Annual phytoplankton production in a system of shallow temperate estuaries. In *Some Contemporary Studies in Marine Science*. (Barnes, H., ed.). George Allen and Unwin Ltd., London, pp. 689-716.